Journal of The Electrochemical Society, **163** (14) D780-D786 (2016)
0013-4651/2016/163(14)/D780/7/$33.00 © The Electrochemical Society

Codeposition of Particles: Role of Adsorption of the Electroactive Species

L. N. Bengoa,[a,b,z] P. Pary,[a,b] and W. A. Egli[a]

[a] *Centro de Investigación y Desarrollo en Tecnología de Pinturas-CIDEPINT (CICBA-CONICET), 1900 La Plata, Argentina*
[b] *School of Engineering, Universidad Nacional de La Plata, 1900 La Plata, Argentina*

Cu-Al_2O_3 composite coatings were obtained from a 0.2 M Cu^{2+} and 0.6 M monosodium glutamate electrolyte whose pH was adjusted at different values in the 3–10 range. Particle charging behavior was studied through ζ-potential measurements and the potential of zero charge of the electrode was determined using Electrochemical Impedance Spectroscopy. Scanning Electron Microscopy was used to characterize coatings surface and to detect particle incorporation. The wt% of alumina in the deposits was estimated using Energy Dispersive Spectroscopy performed on their cross section. Under these experimental conditions high incorporation of particles into the copper matrix was observed, which was ascribed to the increased Cu^{2+} adsorption on Al_2O_3 surface induced by the presence of glutamate in the electrolyte. It was found that hydration forces strongly influence the codeposition of particles as proposed by Fransaer et al. The results were used to identify the relevant steps in the process and to develop a semi-empirical model.
 [DOI: 10.1149/2.0721614jes]

Manuscript submitted August 10, 2016; revised manuscript received October 14, 2016. Published November 8, 2016.

Electrocodeposition is a well-known process in which inert particles are embedded in a metallic matrix during electrodeposition. The result of this process is a metallic coating containing micro or nano particles of a different material dispersed throughout the deposit, i.e. a composite coating. In order to produce such coatings, particles are added to the plating bath and are kept in suspension either by mechanical or ultrasonic agitation or by the addition of a dispersant agent. The main advantage of this technique is that it provides an effective method to obtain deposits with unique properties, resulting of the combination of the particles' characteristics (ceramic, metallic, organic) with those of the electrodeposited metal. As a consequence composite coatings have several applications, among which the development of wear and corrosion resistant deposits,[1,2] self-lubricating coatings[3,4] and dispersion strengthened coatings[5] are the most important, as has been already stated by Celis et al.[6] However, these are just some uses of the codeposition technique that have been reported so far; several new applications have been envisaged in the last decade[7] and many others are still to be developed.[8,9]

Although the incorporation of particles during electrodeposition has been known since the advent of the electroplating industry[10,11] the first attempt to produce a technological coating using this method dates from 1928.[12] However, it was not until the sixties that a strong interest in this field emerged. Since then, several authors have studied the codeposition of particles trying to give an insight into the mechanism of this process and to develop novel coatings with special properties. During the last decades a large number of different metal-particle systems have been investigated: Cu-Al_2O_3,[13–16] Ni-Al_2O_3,[17–21] Ni-WC,[22] Ni-SiC,[1,2,23] Ni-P,[24] Ni-W,[25] Ni-W-P,[24] Ni-W-P-SiC,[24] Ni-P-diamond,[26] Cr-SiC, Cr-C,[5] bronze-graphite,[4,27,28] Ni-oil-containing microcapsules,[3] Zn-TiO_2.[29,30]

As was stated before, many researchers have focused their efforts on understanding the influence of different variables in the amount of incorporated particles. Their results show that the factors affecting this process include particle properties (material, size and shape), bath composition (constituents, pH and additives) and deposition conditions (current density, particle concentration, agitation, etc.).[10,31] Based on their findings, many authors have proposed different mechanisms to account for the behavior found experimentally.[32–39] However, none of the models developed proved to be useful in making consistent predictions. Furthermore, some results obtained are contradictory and cannot be interpreted by any of the existing models. For example, Bund and Thiemig[15,20] found that particle content was higher in electrolytes where particles were negatively charged. Since they carried out their experiments under potential conditions for which the electrode also had a negative charge, these results could not be interpreted using Guglielmi's model which states that particle incorporation occurs via an electrophoretic mechanism. Likewise, all existing models failed to explain the incorporation behavior observed by Hovestad et al. when surfactants were added to the solution.[40]

Despite the discrepancies among the different proposed mechanisms, it has been established that the codeposition of particles involves the following steps:[9,41]

1. Ion adsorption on particles surface, including electroactive species (formation of the ionic cloud).
2. Convective-diffusive transport of particles from the solution's bulk to the surface of the electrode.
3. Adsorption of particles at the cathode (Langmuir Isotherm).
4. Final incorporation to the growing deposit.

Several attempts have been made to describe the mechanism through which the particles are entrapped in the metallic matrix. In fact, the main differences between the existing models rely on this step. For example, the mechanism proposed by Celis et al.[34] suggests that the adsorption of the electroactive species onto the surface of the particles, is a fundamental step of the codeposition process. The authors applied their model to interpret the experimental data gathered for the Cu-Al_2O_3 system. In their work, a regular copper sulfate electrolyte (pH = 0.3) was used to obtain the composite deposits. However, the adsorption of Cu^{2+} on alumina surface is strongly pH-dependent,[42] being insignificant at pH values lower than 5.[43,44] This could explain the low amount of particles embedded that has hitherto been reported. Preliminary studies carried out in our laboratory at pH ≈ 4 in the same electrolyte, indicated that an increase in pH promotes the incorporation of alumina into the copper matrix, in accordance with the hypothesis of Celis et al. Due to copper oxide/hydroxide precipitation,[45] this pH value could not be surpassed to further verify this postulate. Therefore, literature was revised in order to find compounds capable of complexing Cu^{2+} and making it possible to vary the pH of the solution over a wider range. It was found that glutamate ion (**Glu^{2-}**, $C_5H_7NO_4^{2-}$) not only fulfills this task[46] but also promotes adsorption of Cu^{2+} on alumina[44,47] through the formation of ternary surface complexes. In acidic suspensions (pH < 7), glutamate ions bond to the positively charge sites of alumina's surface through its γ-carboxyl group, leaving the cation free to coordinate with another **Glu^{2-}** and to interact with the electrode (complex SL, Fig. 1a), whereas in alkaline conditions Cu^{2+}-**Glu^{2-}** complexes interact with Al_2O_3 through the metallic ion (complex SM, Fig. 1-b).[44,47] Based on this evidence, it seems logical to think that the use of this system in codeposition experiments could help to give a step forward in understanding this phenomenon. Moreover, since **Glu^{2-}** promotes the adsorption of Cu^{2+} on alumina, the addition of this organic compound to the electrolyte might be useful to identify the role of this step on

[z] E-mail: l.bengoa@cidepint.gov.ar

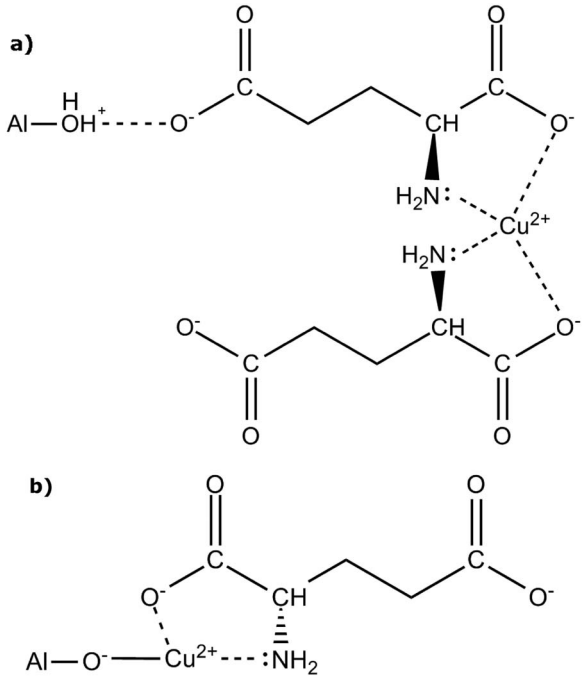

Figure 1. Chemical structure of Cu^{2+}-$\mathbf{Glu^{2-}}$ complexes formed at the surface of Al_2O_3. (a) SL complex and (b) SM complex.[44]

the codeposition process. This kind of approach has never been used before in the study of this phenomenon.

The aim of this work is to give an insight into particle codeposition mechanism, giving special attention to the influence of bath composition and adsorption of the electroactive species on particle incorporation into the metallic matrix. To that end, composite copper-alumina deposits were obtained from a Cu^{2+}-$\mathbf{Glu^{2-}}$ electrolyte at different pH values and current densities. Alumina content was measured and correlated with electrochemical parameters to develop a semi-empirical model.

Materials and Methods

α-Al_2O_3 particles (Alcoa A2G) with a specific BET-surface of 0.93 m^2g^{-1}, determined by N2 adsorption (Micromeritics ASAP 2020 V1.02 E), were used throughout this study. According to XRD measurements, these particles have a 97.5 % purity containing traces of $NaAl_{11}O_{17}$ (2 %) and $Al_3Na_7O_8$ (0.5 %). No purification treatment was applied to this sample. The size distribution of these particles shown in Fig. 2 was measured using a Malvern Mastersizer 2000. The latter has two peaks, which are located at 0.54 μm and 5.6 μm.

Electrodeposition experiments were carried out in a three-electrode cell using an EG&G Princeton Applied Research potenciostat-galvanostat (model 273A) controlled by Corrware2 software. Flat copper substrates with an active area of 0.2 cm^2 were placed vertically inside the cell and used as cathodes. A flat counter electrode of pure copper (14.4 cm^2) and a saturated calomel reference electrode (SCE) were used. All potential values reported in this work are versus this reference electrode. Based on the results of Pary et al.,[48] a 0.2 M $CuSO_4$ (Cicarelli, 100 %) and 0.6 M $NaC_5H_8NO_4$ (Cicarelli, 99 %) solution was prepared, whose pH was adjusted between 3 and 10 by addition of either H_2SO_4 or KOH. Cu-Al_2O_3 deposits were obtained galvanostatically at different pH values at various current densities (-10 A $dm^{-2} < j < -1$ A dm^{-2}) and the electrode potential (E) was registered. Deposition time, calculated using Faraday's law assuming an efficiency of 100 %,[48] was set to reach a 20 μm thickness. A particle concentration of 20 g L^{-1} and a temperature of 60°C were used in all codeposition experiments. To ensure a good particle dispersion, the suspension was stirred for two hours previous to deposition experiments. Likewise, particles were kept in suspension by constant mechanical agitation using a magnetic stirrer (800 rpm) while deposition was carried out. It is important to recall that magnetic stirring generates poorly defined and hardly reproducible hydrodynamic conditions. Therefore, studies using electrodes with well-known hydrodynamics (RDE, RCE) should be performed in the future.

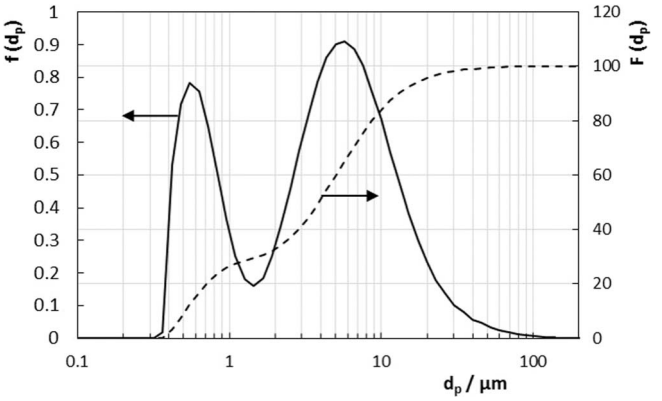

Figure 2. Volume-based normal ($\mathbf{f(d_p)}$) and cumulative $\mathbf{F(d_p)}$ particle size distribution vs particle diameter of α-Al_2O_3 used in codeposition experiments. Measurements were carried out in water.

To characterize particles charging behavior, their isoelectric point (IEP) was determined by dynamic light scattering using a Brookhaven 90 Plus/ Bi-MAS analyzer. Alumina particles were dispersed in a 10^{-3} M KCl solution to a concentration of 0.5 g L^{-1} and ζ-potential was measured in the pH range 4.5–9, which was adjusted with KOH or HCl. Furthermore, the same measurements were carried out in a diluted Cu^{2+}-$\mathbf{Glu^{2-}}$ electrolyte with 0.01 M Cu^{2+} and 0.2 M $\mathbf{Glu^{2-}}$ concentration to which 0.2 g L^{-1} of Al_2O_3 was added (pH range from 3 to 10). This dilution is necessary since both the high ionic strength of the bath and particle concentration used in deposition experiments hinder the determination of ζ-potential values.[29,49] $\mathbf{Glu^{2-}}$ concentration was set to 0.2 M to keep the speciation unchanged (determined using MEDUSA software).

The potential of zero charge (E_{PZC}) of the copper substrates in the Cu^{2+}-$\mathbf{Glu^{2-}}$ electrolyte was determined using electrochemical impedance spectroscopy (EIS), performed in diluted electrolytes (0.01 M Cu^{2+}, 0.2 M $\mathbf{Glu^{2-}}$).[50,51] First, impedance spectra at open circuit (E_{OC}) potential were recorded in the frequency range of 65,5 kHz–0.1 Hz applying an AC disturbance signal of 8 mV. From these results, several frequencies were chosen following the procedure of Ter-Ovanessian et al.[52] and single-frequency EIS measurements were carried out sweeping the electrode potential from 0.10 V to −0.50 V (0.02 V steps). Impedance values were corrected by subtraction of the solution resistance[50,51] and differential capacitance (C_{diff}) was then calculated according to Eq. 1. Since the E_{PZC} corresponds to the potential at which C_{diff} reaches its minimum,[51] its value was obtained from C_{diff} vs E curves.

$$C_{diff} = \frac{Y''}{\omega} \qquad [1]$$

where Y'' is the imaginary part of the electrode admittance and ω is the frequency at which the admittance was determined.

Scanning electron microscopy (SEM) was used to examine the morphology of the coatings and the particle content (Quanta200 FEI microscope). In order to observe coatings cross section, samples were embedded in an epoxy resin, ground using 80 to 2500 grade silicon paper and polished with 6 μm and 1 μm diamond paste. The alumina content in the deposit was estimated through energy dispersive spectroscopy (EDS) analysis performed at a 1500× magnification in an area equal to the visible cross section of the coating. Values reported in this study are the average of at least three measurements.

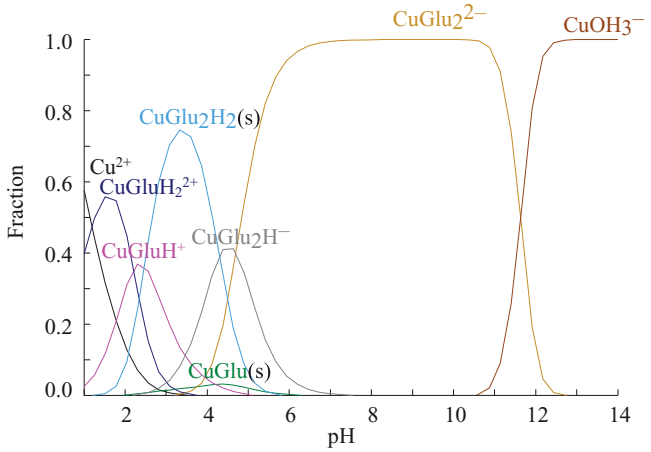

Figure 3. Species distribution of the Cu^{2+}-**Glu^{2-}** system in an alumina-free electrolyte: 0.2 M Cu^{2+} and 0.6 M **Glu^{2-}**.

Results

The **Glu^{2-}**/Cu^{2+} ratio chosen, ensures the formation of complexes both in the solution and at the alumina surface and avoids the inhibition of Cu^{2+} adsorption that can be caused by an excess of ligand.[47] According to equilibrium calculations made with MEDUSA software (equilibrium constants and potentials were taken from Refs. 45,46), the main species present in the solution changes with pH (Fig. 3) and, consequently, deposition potential might vary too. It is worth remarking that Fig. 3 describes the speciation in an alumina-free system and that surface complexes which form onto Al_2O_3 particles (Fig. 1) at each pH differ from those found in solution.[44,47]

Fig. 4 shows the influence of current density on the alumina content of copper coatings at different pH conditions. The same trend was observed for all pH values higher than 3 considered in this study. In particular, virtually no differences were observed between results obtained at pH = 6 and 8, suggesting that the electrochemistry of the system (reactions involved, ζ-potenial and adsorbed complexes) is the same at both pH values. Under these conditions (pH > 3), particle content decreased sharply as current density was raised, becoming negligible for $j < -5$ A dm^{-2}. Similar results have been previously reported for many metal-particle combinations.[27,29,53] On the other hand, at pH = 3 relatively high alumina contents were measured in the whole current density range. For this pH value, a maximum in particle incorporation appeared at $j = -2.5$ A dm^{-2}. This kind of behavior has already been observed by several authors[9,11,13,37,54,55] and

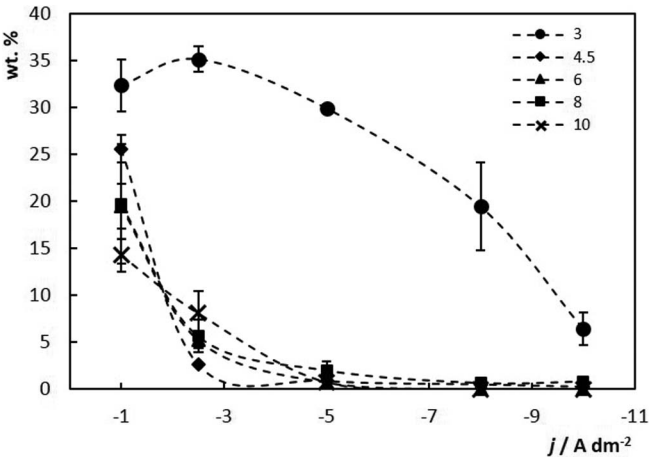

Figure 4. Variation of Al_2O_3 wt% with current density at different pH values. Content of particles was measured on the cross section of the coatings.

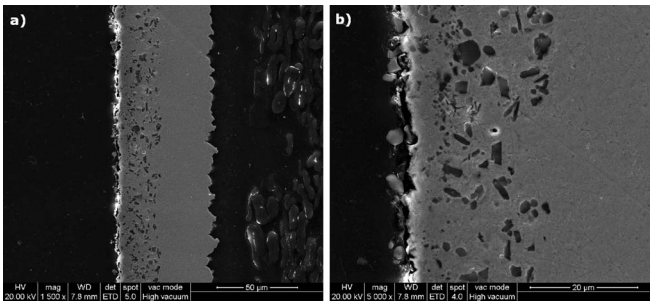

Figure 5. Cross section of Cu-Al_2O_3 deposit obtained at pH = 3 and $j = -1$ A dm^{-2}: (a) 1500 X and (b) 5000 X.

the presence of a maximum in the content vs *j* curve has been a topic of discussion for many years. Further information on this matter is given in the following paragraphs. It is noteworthy that the wt% of alumina registered in the copper deposits, widely surpassed values reported by other authors[11,13,15,34,56,57] (less than 10 wt% for similar bath particle concentrations and current densities). Considering that the presence of glutamate in the bath favors the uptake of Cu^{2+} on alumina surface even in low pH solutions,[44,47] these results suggest that adsorption of the electroactive species is a relevant step in codeposition in agreement with Celis et al. postulate.[34] Another important feature of the deposits obtained, is that particles were homogeneously distributed throughout the metallic matrix (Fig. 5), which may be indicative of an adequate dispersion in the solution. The latter can be ascribed to an increase in steric repulsion between particles caused by the presence of Cu^{2+}-**Glu^{2-}** complexes adsorbed on alumina surface.[58,59] According to Guglielmi's model,[33] the entrapment of particles occurs via an electrophoretic mechanism. This means that, for the particles to reach the electrode, a favorable electrostatic interaction must exist between these elements. Therefore, it is relevant to characterize the charging behavior of both particles and electrode at the experimental conditions used for deposition experiments. ζ-potential measurements in a diluted Cu^{2+}-**Glu^{2-}** electrolyte (Fig. 6) indicated that particles are positively charged in solutions with pH < 3.5, probably due to low copper complexes uptake.[47] As a consequence, ζ-potential sign is likely governed by the protonation of hydroxyl groups since IEP (10^{-3} M KCl) of Al_2O_3 used in this study is located at pH = 5.8 (Fig. 6). It is important to remark that despite this, the amount of adsorbed Cu^{2+} in the presence of **Glu^{2-}** is significant compared to adsorption in **Glu^{2-}**-free electrolytes,[44,47] which could explain the high particle contents measured. Another plausible cause of the positive ζ-potential values, is the protonation of the γ-carbonyl group

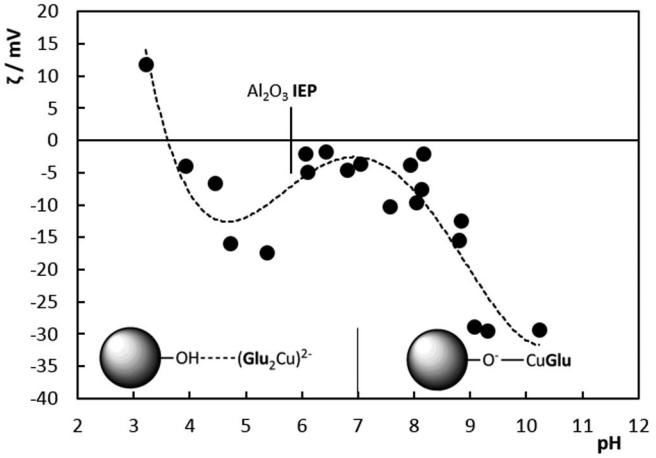

Figure 6. ζ-potential of Al_2O_3 particles determined in a 0.01 M Cu^{2+}, 0.2 M **Glu^{2-}** electrolyte.

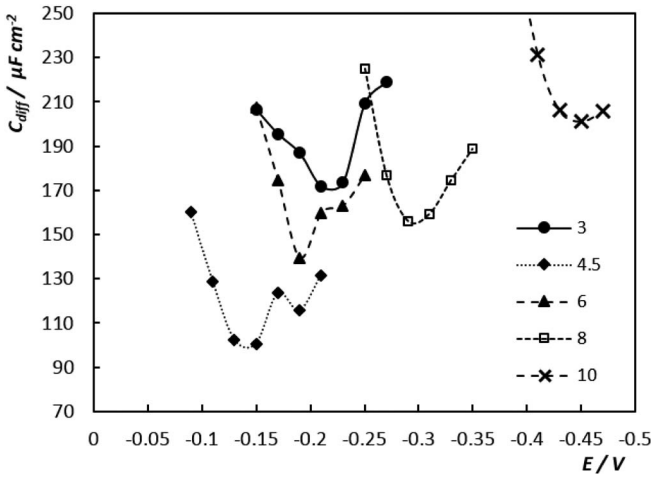

Figure 7. C_{diff} vs E curves from which E_{PZC} values were obtained.

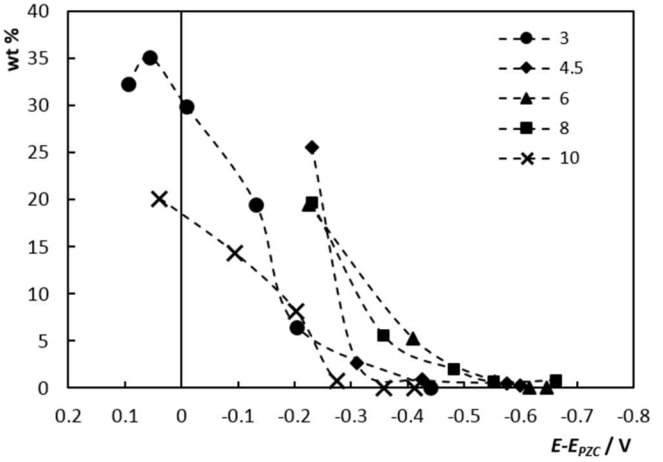

Figure 8. Dependence of Al_2O_3 wt% with the difference E-E_{PZC}.

(pKa = 4.3) of adsorbed **Glu^{2-}** molecules (see Fig. 1). A comment regarding the IEP (10^{-3} M KCl) of the alumina sample is necessary: although its value differs from the typical IEP reported for Al_2O_3 particles (8-9[60–62]), such a behavior has already been observed and has been ascribed to the presence of impurities in the sample.[63]

As the pH increases from 3 to 5, so does the uptake of Cu^{2+} complexes,[47] leading to a decrease in ζ-potential due to the negative charge of SL type complex. A further increase in pH yields a decrease in ζ absolute value and the cause of this reduction is not entirely clear. According to results reported by other authors, copper adsorption in a 0.0005 M Cu^{2+} solution is maximum at pH = 6.[47] It is possible that at the concentration used in this work for ζ-potential measurements (0.01 M Cu^{2+}) the maxima in copper uptake is located at lower pH values (≈5), which could explain the variation of ζ found. Lastly, for pH > 7.5 a continuous decrease in ζ-potential is observed. Considering that the adsorption of complexes is hampered to some extent in alkaline conditions,[44,47] this trend can be ascribed to the deprotonation of free hydroxyl groups on alumina's surface. It is worth mentioning that SO_4^{2-} ion adsorption onto alumina surface has been reported. According to Kosmulski et al.[64] sulfate ions adsorb on particles surface yielding a negative ζ-potential. This effect is stronger at low pH values, i.e. ζ absolute value decreases as pH increases. Since the measured ζ of alumina is positive at low pH values, it can be assumed that SO_4^{2-} ions does not play an important role in a Cu^{2+}-**Glu^{2-}** electrolyte. This can be the result of the higher stability of surface complexes, which inhibit sulfate adsorption

Fig. 7 shows the C_{diff} vs E curves recorded at each pH considered in this study while the E_{PZC} values obtained are summarized in Table I together with the E_{OC}. As expected, these potentials vary considerably with pH. A steady decrease of E_{PZC} is observed as the pH increases from 4.5 to 10. The same behavior has been reported for various substrates such as Pt,[65] Au, Ag[66] and Cu,[67] which has been ascribed to an increase in the amount of adsorbed OH^- at the electrode surface. However, E_{PZC} at pH = 3 turned out to be more cathodic than at 4.5. This inversion in the usually observed trend in simpler composition solutions, could be caused by **Glu^{2-}** adsorption onto copper electrode.[68,69] The latter may be higher at lower pH values due to a smaller OH^- concentration and a higher excess of ligand, since at pH = 3 the main species in solution is a 1:1 Cu^{2+}-**Glu^{2-}** complex.

Table I. E_{OC} and E_{PZC} of copper electrodes at various pH values.

pH	E_{OC}/V	E_{PZC}/V
3	0.02	−0.22
4.5	−0.07	−0.15
6	−0.12	−0.19
8	−0.21	−0.29
10	−0.31	−0.45

To clarify the effect of charge of the electrode on particle incorporation, alumina contents were plotted against the difference between the deposition potential and E_{PZC}. The former was taken from the data recorded during electrodeposition experiments. Fig. 8 clearly shows that, regardless of the pH of the electrolyte, the amount of particles in the coating diminishes when E departs from E_{PZC}. Moreover, the decrease in alumina content is more abrupt for pH values at which particles possess a higher surface charge (4.5 and 10), than for those at which the ζ-potential is close to 0 (6 and 8). This behavior and the similarities between results obtained in the pH range 6-8, suggest that electrode-particle electrostatic interactions may be involved in the codeposition process. Comparison of Figs. 4 and 8, further clarifies the variation of Al_2O_3 wt% with current density detailed before. For example, it shows that at the working current densities the potential values for pH 3 and 10 are closer to the E_{PZC} than for the other pH conditions. This could explain the higher particle incorporation observed at pH = 10 for $j < -2.5$ A dm^{-2} and at pH = 3 for the whole j range. To verify the behavior observed in Fig. 8 for pH 4.5-10, a deposit was obtained from a pH = 3 electrolyte at a current density for which E-$E_{PZC} \approx -0.45$ V. At this E-E_{PZC} value, no particles were detected in the Cu matrix for any of the pH values considered in this study (Fig. 8).

Even though it was stated that electrostatic interaction might play some role in the codeposition process, the high alumina contents measured at pH = 4.5 where both particle and electrode are negatively charged indicate that it is not a relevant step. Furthermore, the sharp decrease in particle incorporation as E becomes more cathodic observed at pH = 3, supports this idea (positively charged particles, see Fig. 6). Hence, it can be concluded that the electrophoretic movement contributes to the codeposition of particles, as previously reported,[70] though it is not a fundamental factor for their entrapment. In fact, Fransaer et al.[37] established that the electrophoretic force can be neglected when deposition takes place on a rotating disk electrode. However, years later they also found that the predominant force between a silica particle and a copper electrode was electrostatic in nature.[71] Moreover, Soccol et al. found that the ζ-potential strongly influences the codeposition of brownian particles.[70] It is then clear that the relevance of this kind of interaction is different for each case.

The results obtained at pH = 3 suggest that the maximum amount of particles is reached in the vicinity of E_{PZC}. To verify the position of this maxima, deposition was performed in a pH = 10 electrolyte at $j = -0.7$ A dm^{-2}. At this current density $E \approx E_{PZC}$ and the content of alumina measured was the highest for this pH value (Fig. 8). Similar experiments could not be carried out at other pH values since E_{OC} is too close to E_{PZC} (Table I). The dependence of particle content with electrode potential observed in these experiments is in

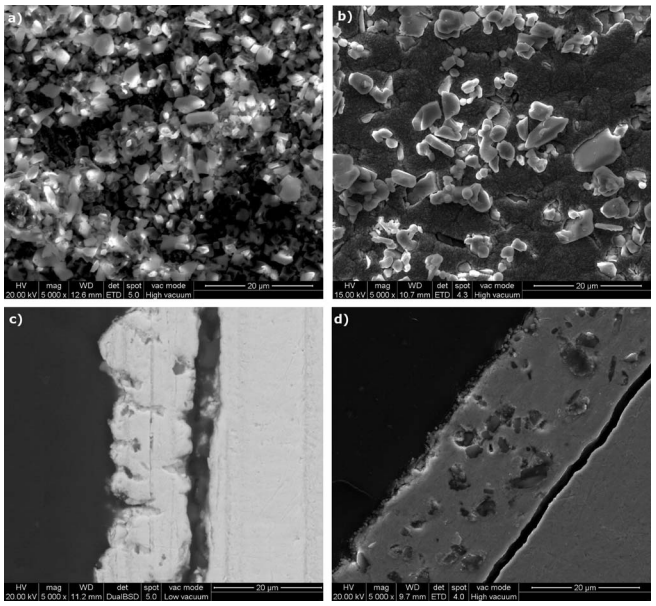

Figure 9. Surface and cross section of Cu-Al_2O_3 deposit obtained from (a) and (c) a copper sulfate bath at pH ≈ 4; (b) and (d) a Cu^{2+}-**Glu^{2-}** bath at pH = 4.5 (5000 X).

agreement with the results of Fransaer et al.,[37] who also found that the highest incorporation rate is achieved when $E \approx E_{PZC}$. They ascribed this behavior to the presence of a hydration layer at the surface of the electrode, which hinders the approach of particles to the growing metal. Studies performed afterwards with an atomic force microscope[71–73] confirmed the presence of this layer and the particle-electrode gap that it creates. It is known that when the electrode posses a zero net charge, i.e. $E = E_{PZC}$, water molecules are loosely attached to its surface and can be easily removed by an approaching particle. Therefore, at this condition particle incorporation is maximum.

Discussion

Some conclusions on the electrocodeposition process can be reached based on the information gathered during this study. First, adsorption of the electroactive species onto the particles surface is determining for their subsequent incorporation in the deposit, in accordance with Celis et al.[34] This stems from the high alumina contents achieved after addition of **Glu^{2-}** to the electrolyte, which promotes Cu^{2+} uptake. Moreover, it was found that in the presence of this organic compound, the excess of particles at the surface of the deposit is less than the one observed in coatings deposited from a sulfate bath at pH ≈ 4 (Fig. 9). The latter suggests that **Glu^{2-}** makes the Cu^{2+}-Al_2O_3 bond stronger favoring entrapment and reducing the 'riding' effect which pushes the particles toward the electrolyte-metal interface.[57,72–74]

Additionally, the results support the role of the repulsive hydration force previously proposed by Fransaer et al. This force reaches a minimum value at E_{PZC},[37,39] allowing the particles to come closer to the electrode surface. When the distance between them is small, attractive forces (such as dispersion forces) keep the particles attached to the growing deposit and, consequently, incorporation is maximum at this potential. The fact that the maximum alumina content at pH = 3 is shifted from the E_{PZC} can be attributed to intrinsic uncertainties of the method used to determine this parameter. Taking into account that high alumina contents were attained even in conditions at which particles and electrode have charges of the same sign, it is obvious that particle entrapment does not occur through an electrophoretic process as suggested by Guglielmi. Since adsorption of the electroactive species plays a major role in codeposition, it is likely that particles are embedded as a result of the reduction of adsorbed ions on their surface.[34]

Based on the shape of the curve obtained for pH = 3 (Fig. 8), a semi-empirical mathematical model was proposed, in which the dependence of alumina content with E-E_{PZC} is described by a Gaussian function (Eq. 2). In this equation, W_{max} represents the maximum content that can be achieved at a given pH. By fitting and extrapolation of the model to $E = E_{PZC}$, it was found that this parameter lies between 16–41 wt% in the pH range considered in this work. As regards the κ coefficient, the results indicated that its value is strongly dependent on the ζ-potential (Eq. 3, $r^2 = 0.9993$), which demonstrates the influence of particles surface charge on the process. From this quadratic dependence it can be inferred that an increase in surface potential, regardless of sign, hampers the approximation of particles to the electrode surface as the potential steps away from E_{PZC}. This effect could be caused by the hydration layer of particles: water molecules polarization would increase as the surface charge of the particle increases, regardless of its sign. Thus, water molecules become more strongly attached to the particles, which leads to an increase in the hydration force and hinders real contact between particles and the electrode surface.

$$wt\% = W_{max} e^{-\kappa(E-E_{PZC})^2} \quad [2]$$

$$\kappa = 0.07\zeta^2 + 1.03\zeta + 15.29 \quad [3]$$

Fig. 10 shows that the proposed mathematical expression is capable of reproducing the main trends observed in the experimental data in the range $-0.70\ V < E\text{-}E_{PZC} < 0.10\ V$. For instance, at E-$E_{PZC} < -0.30$ V the calculated alumina content is higher at pH = 6 than for other pH values, being almost zero at pH = 3 and 10. Likewise, Al_2O_3 wt% is higher for pH = 3 than for pH = 10 at $E = E_{PZC}$, in agreement with experimental results. The adequacy of this model to describe the Cu-Al_2O_3 in a glutamate bath is evidenced by the fact that $r^2 > 0.92$ for the whole pH range, except for pH = 4.5. The latter, together with its mathematical simplicity and the low number of parameters to be fitted, may make it a useful tool to describe the codeposition of particles. Another interesting feature of the W_{max} values obtained from the fitting procedure, is that this parameter varies with pH in a similar way to ζ-potential (Fig. 11). This suggests that the magnitude of the surface charge of the particles has some influence on codeposition even when the electrode bears no charge. However, since it was not possible to obtain deposits at E_{PZC} for all pH values under study, this trend could not be confirmed with experimental data. Further studies will be carry out in the future to find particle-metal systems for which deposition at the potential of zero charge is feasible in order to verify the relation between W_{max} and ζ.

Conclusions

Deposition experiments and the analysis carried out in this study have allowed the identification of the steps involved in the codeposition of particles present in an electrolytic bath. It was shown that adsorption of the electroactive species on the surface of alumina particles, i.e. Cu^{2+}, is a requirement for the successful entrapment of particles in the growing deposit. Moreover, the role of hydration forces was confirmed whereas the electrophoretic movement of particles proved not to be a relevant step in this process. High alumina contents were attained in the presence of **Glu^{2-}**, which indicates that particle incorporation can be significantly improved by addition of compounds that promote adsorption of the electroactive species on the particles surface. This would permit the production of new composites materials via electrolytic deposition. Hence, the results of this work provide a new approach for the design of novel composite materials.

Finally, a semi-empirical model was proposed, capable of reproducing the experimental data obtained during codeposition of Cu-Al_2O_3 coatings on static electrodes from a Cu^{2+}-**Glu^{2-}** electrolyte. Future investigations will be devoted to validation of this model using other metal-particle systems in which the electroactive species

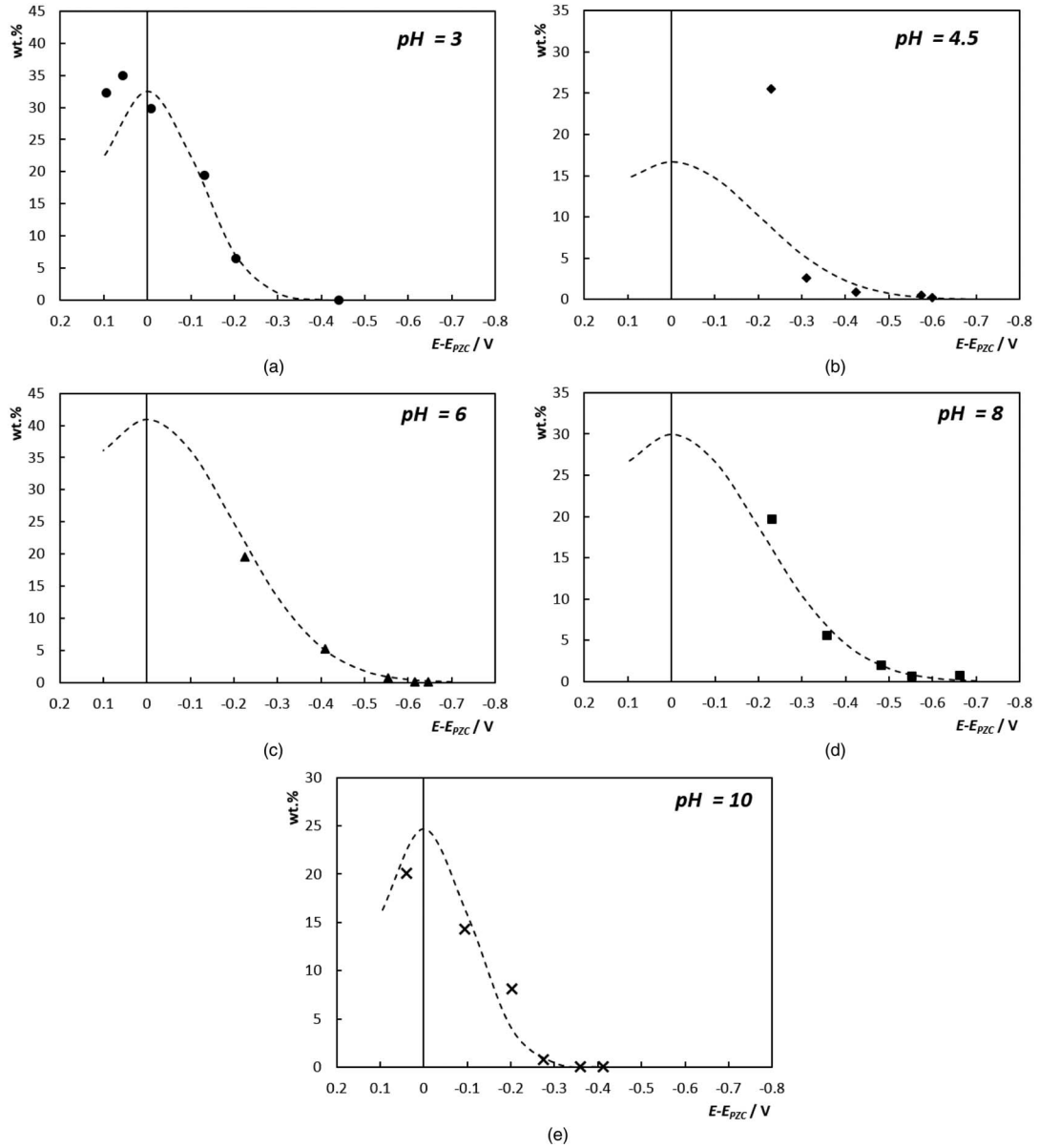

Figure 10. Results yielded by the proposed model in the potential range -0.70 V $< E\text{-}E_{PZC} <$ 0.10 V. The experimental data are also presented for comparison purposes.

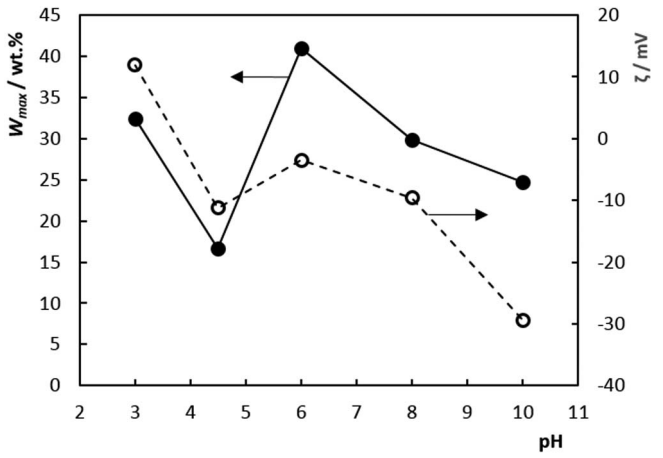

Figure 11. W_{max} and ζ as a function of pH.

readily adsorbs on the particles and under controlled mass transport conditions.

Acknowledgments

The authors would like to acknowledge the financial support given by Comision de Investigaciones Científicas de la Provincia de Buenos Aires (CICPBA, N° 833/14), Consejo Nacional de Investigaciones Científicas y Técnicas (CONICET, PIP N° 00737) and Universidad Nacional de La Plata (UNLP, *N*° 11/I201) for this research. L.N. Bengoa wishes to thank SIDERCA S.A.I.C and CONICET for a Ph.D grant (D.C. 1517). P. Pary thanks CONICET for Ph.D grant D. 1189.

References

1. M. Vaezi, S. Sadrnezhaad, and L. Nikzad, *Colloids Surf., A*, **315**, 176 (2008).
2. M. Lekka, N. Kouloumbi, M. Gajo, and P. Bonora, *Electrochim. Acta*, **50**, 4551 (2005).
3. S. Alexandridou, C. Kiparissides, J. Fransaer, and J. P. Celis, *Surf. Coat. Technol.*, **71**, 267 (1995).

4. M. Ghorbani, M. Mazaheri, and A. Afshar, *Surf. Coat. Technol.*, **190**, 32 (2005).
5. M. Gines, F. Williams, and C. Schuh, *Journal of Applied Surface Finishing*, **2**, 112 (2007).
6. J. Celis, J. Roos, C. Buelens, and J. Fransaer, *Trans. Inst. Met. Finish.*, **69** (1991).
7. M. Musiani, *Electrochim. Acta*, **45**, 3397 (2000).
8. V. N. Tseluikin, *Prot. Met. Phys. Chem*, **45**, 312 (2009).
9. F. C. Walsh and C. Ponce de Leon, *Trans. Inst. Met. Finish.*, **92**, 83 (2014).
10. A. Hovestad and L. J. J. Janssen, *Electroplating of metal matrix composites by codeposition of suspended particles* (Kluwer Academic /Plenum Publishers, New York, 2005), vol. 38 of *Modern Aspects of Electrochemistry*, chap. 6.
11. C. Buelens, J. P. Celis, and J. R. Roos, *J. Appl. Electrochem.*, **13**, 541 (1983).
12. C. Fink and J. D. Prince, *Transactions of the American Electrochemical Society*, **54**, 315 (1928).
13. V. Stankovic and M. Gojo, *Surf. Coat. Technol.*, **81**, 225 (1996).
14. J. Stojak, J. Fransaer, and J. Talbot, *Review of electrocodeposition* (Wiley-VCH, Germany, 2002), vol. 7.
15. A. Bund and D. Thiemig, *J. Appl. Electrochem.*, **37**, 345 (2007).
16. M. Kim, F. Sun, J. Lee, Y. K. Hyun, and D. Lee, *Surf. Coat. Technol.*, **205**, 2362 (2010).
17. M. Bahrololoom and R. Sani, *Surf. Coat. Technol.*, **192**, 154 (2005).
18. D. Thiemig, A. Bund, and J. B. Talbot, *Electrochim. Acta*, **54**, 2491 (2008).
19. D. Thiemig, R. Lange, and A. Bund, *Electrochim. Acta*, **52**, 7362 (2007).
20. A. Bund and D. Thiemig, *Surf. Coat. Technol.*, **201**, 7092 (2007).
21. T. Borkar and S. P. Harimkar, *Surf. Coat. Technol.*, **205**, 4124 (2011).
22. M. Stroumbouli, P. Gyftou, E. Pavlatou, and N. Spyrellis, *Surf. Coat. Technol.*, **195**, 325 (2005).
23. L. Benea, P. Bonora, A. Borello, and S. Martelli, *Wear*, **249**, 995 (2002).
24. Z. Guo, X. Zhu, and R. Xu, *Acta Metallurgica Sinica (English Letters)*, **20**, 111 (2007).
25. I. Mizushima, P. Tang, and H. Hansen, *AESF SUR/FIN* (2006), p. 758.
26. V. Reddy, B. Ramamoorthy, and P. K. Nair, *Wear*, **239**, 111 (2000).
27. A. Afshar, M. Ghorbani, and M. Mazaheri, *Surf. Coat. Technol.*, **187**, 293 (2004).
28. T. Nickchi and M. Ghorbani, *Surf. Coat. Technol.*, **203**, 3037 (2009).
29. M. K. Camargo, U. Schmidt, R. Grieseler, M. Wilke, and A. Bund, *J. Electrochem. Soc.*, **161**, D168 (2014).
30. M. K. Camargo, I. Tudela, U. Schmidt, A. J. Cobley, and A. Bund, *Electrochim. Acta*, **198**, 287 (2016).
31. A. Hovestad and L. Janssen, *J. Appl. Electrochem.*, **25**, 519 (1995).
32. P. Berçot, E. Peña-Muñoz, and J. Pagetti, *Surf. Coat. Technol.*, **157**, 282 (2002).
33. N. Guglielmi, *J. Electrochem. Soc.*, **119**, 1009 (1972).
34. J. P. Celis, J. R. Roos, and C. Buelens, *J. Electrochem. Soc.*, **134** (1987).
35. J. Valdés, Ph.D. thesis, Columbia University, New York (1987).
36. Y. Eng, Electrocodeposition of metal and colloidal particle composite films onto a rotating cylinder electrode, Ph.D. thesis, Columbia University, New York (1991).
37. J. Fransaer, J. P. Celis, and J. R. Roos, *J. Electrochem. Soc.*, **139**, 413 (1992).
38. B. J. Hwang and C. S. Hwang, *J. Electrochem. Soc.*, **140**, 979 (1993).
39. J. Fransaer, Study of the behaviour of particles in the vicinity of electrodes, Ph.D. thesis, Katholieke Universiteit, Belgium (1994).
40. A. Hovestad, R. J. C. H. L. Heesen, and L. J. J. Janssen, *J. Appl. Electrochem.*, **29**, 331 (1999).
41. C. Low, R. Wills, and F. C. Walsh, *Surf. Coat. Technol.*, **201**, 371 (2006).
42. B. Kasprzyk-Hordern, *Adv. Colloid Interface Sci.*, **110**, 19 (2004).
43. E. Baumgarten and U. Kirchhausen-Düsing, *J. Colloid Interface Sci.*, **194**, 1 (1997).
44. J. P. Fitts, P. Persson, G. E. Brown Jr, and G. A. Parks, *J. Colloid Interface Sci.*, **220**, 133 (1999).
45. M. Pourbaix, *Atlas of Electrochemical Equilibria in Aqueous Solutions* (National Association of Corrosion Engineers, Houston, Texas, USA, 1974), second edn.
46. R. M. Smith and A. E. Martell, *Critical stability constants. Volumen 6-Second Supplement*, vol. 6 (Plenum Press, 1989).
47. G. Micera, L. S. Erre, and R. Dallocchio, *Colloids and Surfaces*, **28**, 147 (1987).
48. P. Pary, L. N. Bengoa, and W. A. Egli, *J. Electrochem. Soc.*, **162**, D275 (2015).
49. M. Kosmulski, P. Dahlsten, P. Próchniak, and J. B. Rosenholm, *Colloids Surf., A*, **301**, 425 (2007).
50. H. R. Zebardast, S. Rogak, and E. Asselin, *J. Electroanal. Chem.*, **724**, 36 (2014).
51. V. D. Jović and B. M. Jović, *J. Electroanal. Chem.*, **541**, 1 (2003).
52. B. Ter-Ovanessian, C. Alemany-Dumont, and B. Normand, *J. Appl. Electrochem.*, **44**, 399 (2013).
53. S. W. Banovic, K. Barmak, and A. R. Marder, *J. Mater. Sci.*, **34**, 3203 (1999).
54. V. Terzieva, J. Fransaer, and J.-P. Celis, *J. Electrochem. Soc.*, **147**, 198 (2000).
55. B. Bahadormanesh and A. Dolati, *J. Alloys Compd.*, **504**, 514 (2010).
56. J. P. Celis, H. J. A. Roos, H. P. , and J. R. , *Anal. Chim. Acta*, **92**, 413 (1977).
57. C. White and J. Foster, *Trans. Inst. Met. Finish.*, **59**, 8 (1981).
58. H. Mollet and A. Grubenmann, *Emulsions - Properties and Production* (Wiley-VCH Verlag GmbH, 2000), chap. 2, pp. 59–104.
59. M. Elimelech, et al., *Surface interaction potentials* (Butterworth-Heinemann, Woburn, 1995), chap. 3, pp. 33–67.
60. A. L. Costa, C. Galassi, and R. Greenwood, *J. Colloid Interface Sci.*, **212**, 350 (1999).
61. J. A. Yopps and D. W. Fuerstenau, *J. Colloid Sci.*, **19**, 61 (1964).
62. G. V. Franks and L. Meagher, *Colloids Surf., A*, **214**, 99 (2003).
63. M. Kosmulski, *Colloids Surf., A*, **222**, 113 (2003).
64. M. Kosmulski, P. Prochniak, and J. B. Rosenholm, *Journal of Colloid and Interface Science*, **338**, 316 (2009).
65. E. Gileadi, S. D. Argade, and J. O. Bockris, *The Journal of Physical Chemistry*, **70**, 2044 (1966).
66. D. D. Bode, T. N. Andersen, and H. Eyring, *The Journal of Physical Chemistry*, **71**, 792 (1967).
67. A. Lukomska and J. Sobkowski, *J. Electroanal. Chem.*, **567**, 95 (2004).
68. I. E. Mironyuk, G. S. Shapoval, V. F. Gromovaya, A. S. Bandurenko, and V. P. Kukhar', *Theoretical and Experimental Chemistry*, **40**, 110 (2004).
69. D.-Q. Zhang, Q.-R. Cai, X.-M. He, L.-X. Gao, and G.-D. Zhou, *Materials Chemistry and Physics*, **112**, 353 (2008).
70. D. Soccol, C. Ntumba-Ngoy, S. Claessens, and J. Fransaer, *J. Electrochem. Soc.*, **161**, D601 (2014).
71. C. Dedeloudis, J. Fransaer, and J. P. Celis, *J. Phys. Chem. B*, **104**, 2060 (2000).
72. C. Dedeloudis and J. Fransaer, *Langmuir*, **20**, 11030 (2004).
73. L. Stappers and J. Fransaer, *J. Electrochem. Soc.*, **154**, D598 (2007).
74. L. Stappers and J. Fransaer, *J. Electrochem. Soc.*, **153**, C472 (2006).